Shaping Planetary Nebulae: Evidence of Magnetic Fields Around Evolved Stars

Marcelo L. Leal-Ferreira
(Argelander Institut für Astronomie, Germany)

Dr. Wouter H. T. Vlemmings
(Onsala Space Observatory, Sweden)

universitätbonn

Argelander-Institut für Astronomie

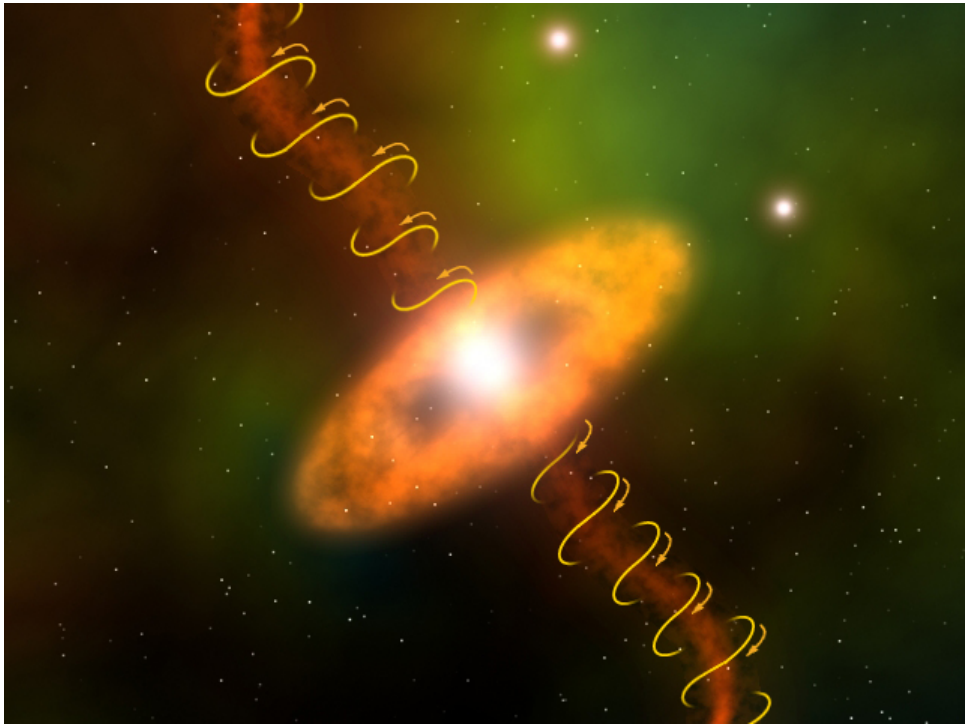

(Artistic impression on W43A; credit: NRAO/AUI/NSF)

DAAD

Overview: Stellar Evolution

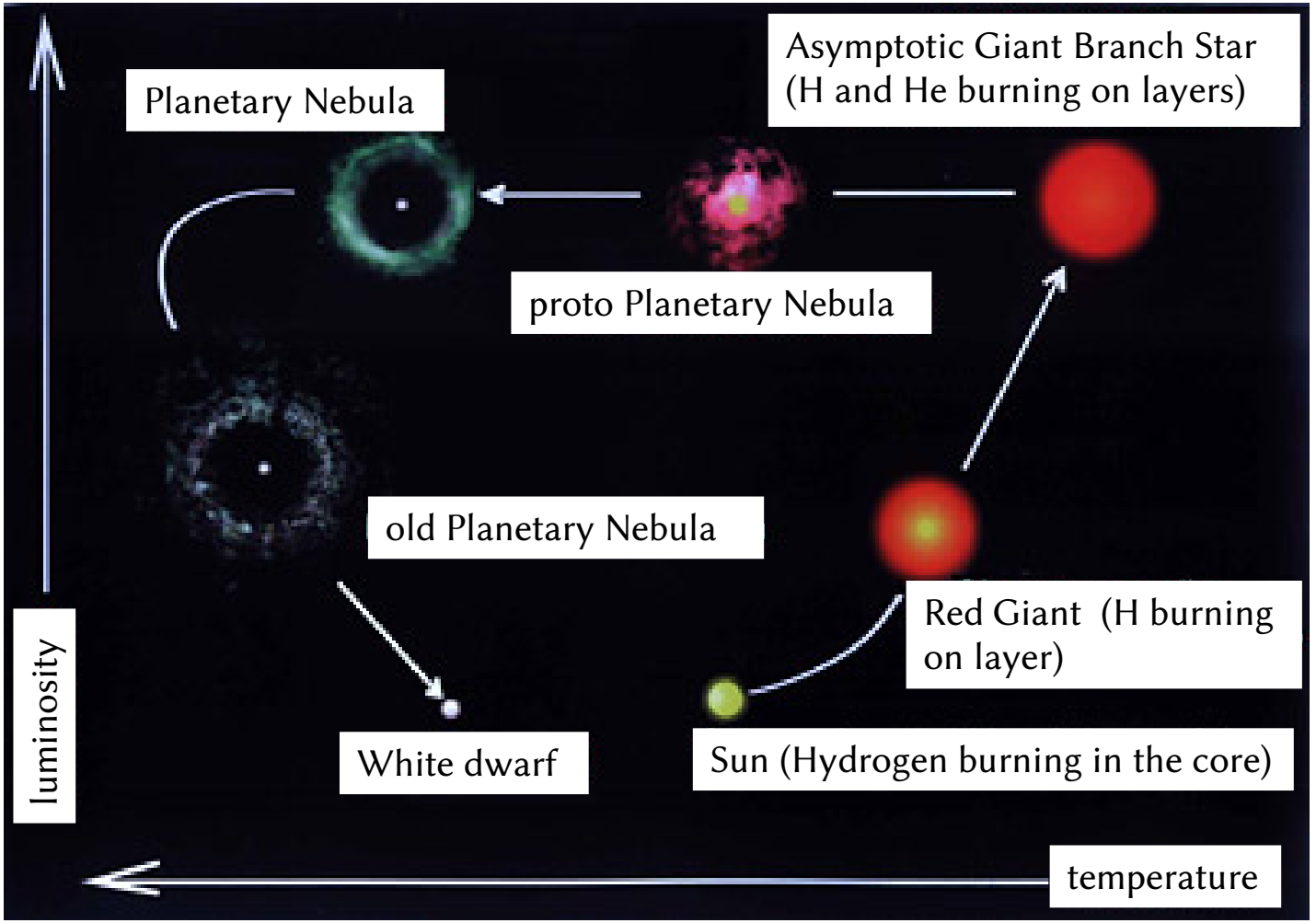

(Credit: Figure adapted from Kwok 2001; Cosmic Butterflies)

Overview: Planetary Nebulae
(Morphology)

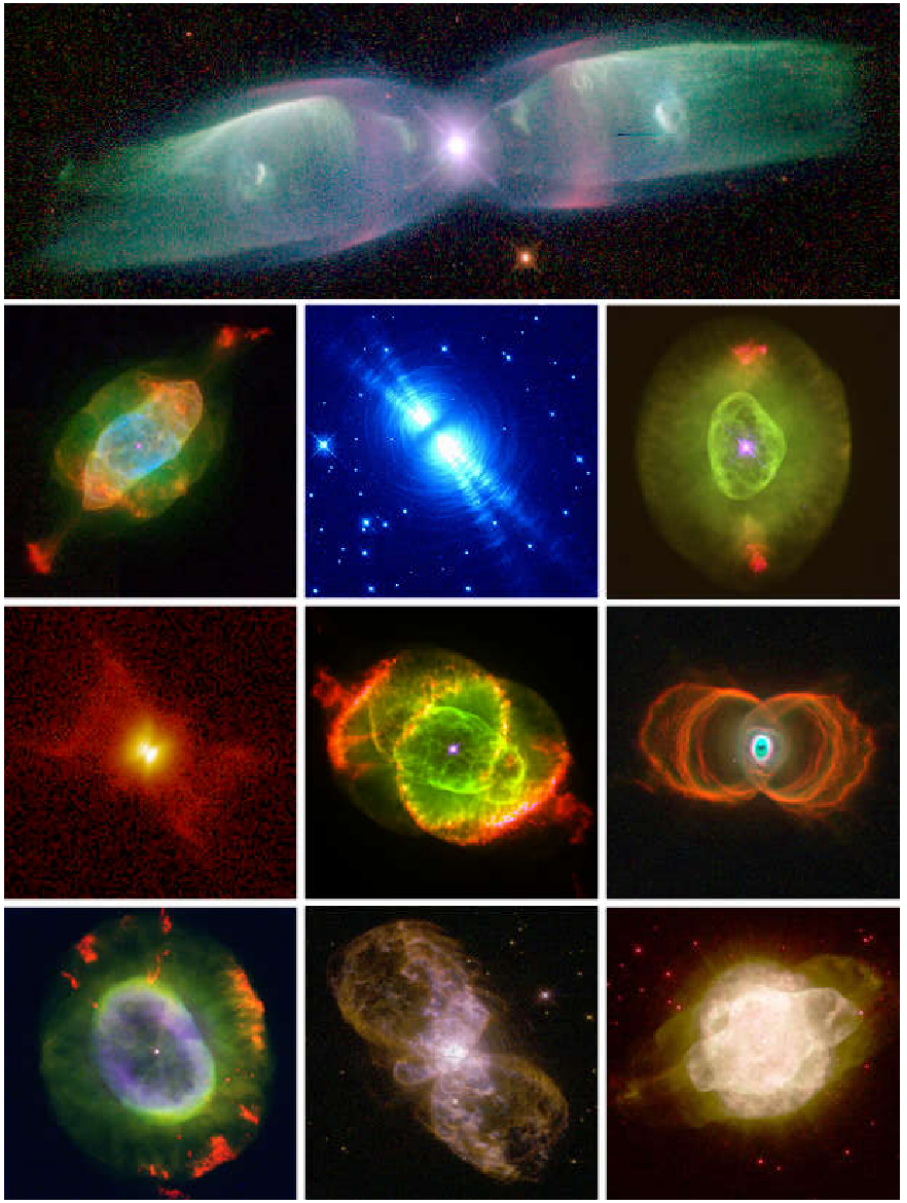

(Credit: Catalog of Planetary Nebula by Bruce Balick)

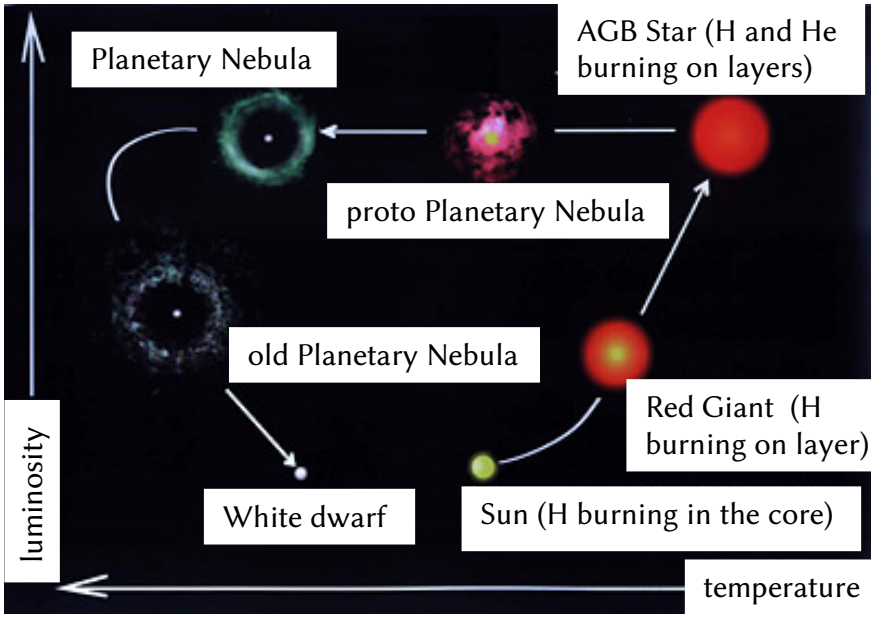

(Credit: Figure adapted from Kwok 2001; Cosmic Butterflies)

Introduction: Shaping an Evolved Star

. Garcia-Segura et al. 1999:
→ "A magnetic field in the AGB winds (...) has a pronounced effect in the resultant morphology of the PN, in general resulting in an elliptical shape."
→ "Strong fields in the AGB wind, combined with a significant rotation, generate highly collimated bipolar PN and jets."

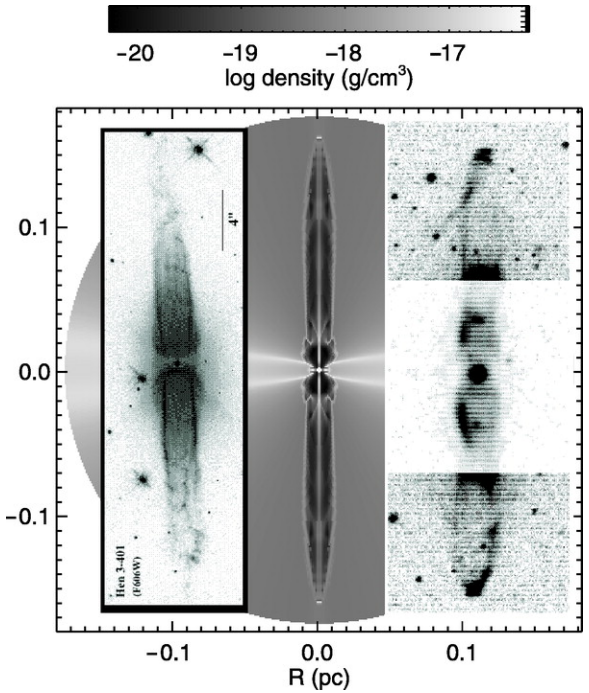

(Credit: Garcia-Segura et al. 2005)

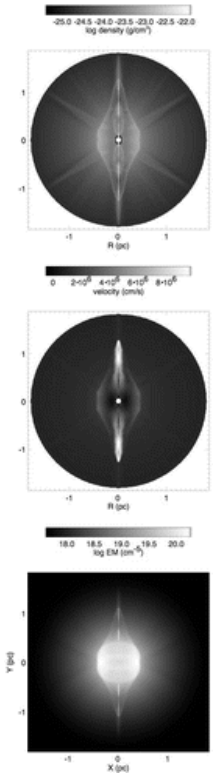

(Credit: Garcia-Diaz et al. 2008)

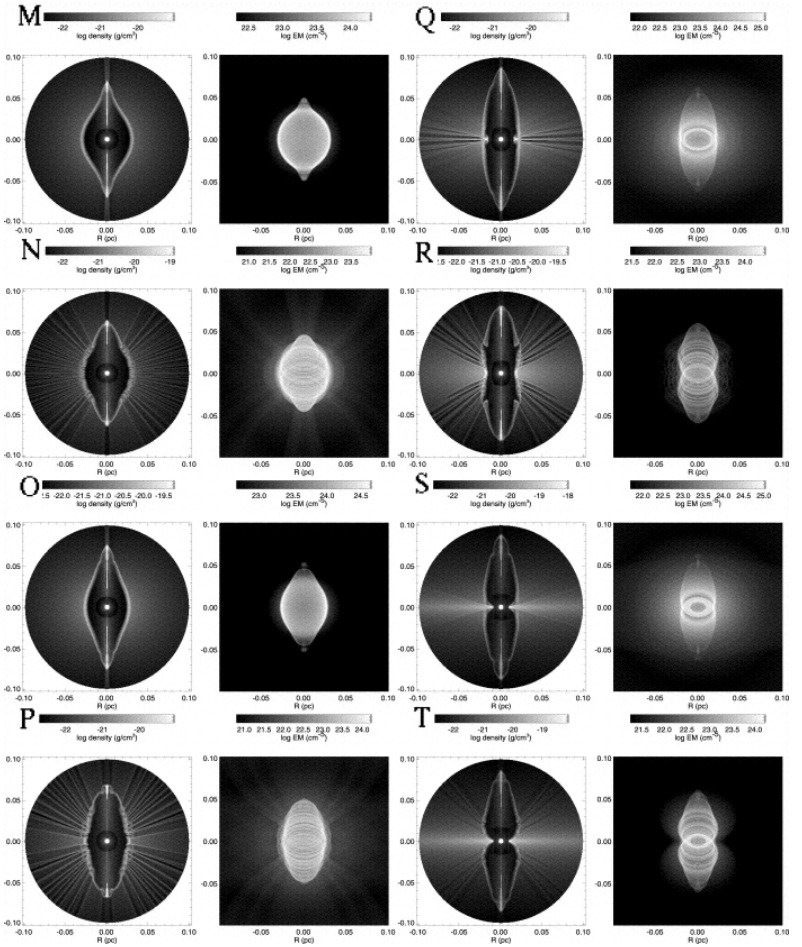

(Credit: Garcia-Segura et al. 1999)

Introduction: Shaping an Evolved Star

. Garcia-Segura et al. 1999:
⟶ “A magnetic field in the AGB winds (...) has a pronounced effect in the resultant morphology of the PN, in general resulting in an elliptical shape.”
⟶ “Strong fields in the AGB wind, combined with a significant rotation, generate highly collimated bipolar PN and jets.”

. Other factors that can influence the shaping of an evolved star:
⟶ A companion to the star, and its tidal forces (heavy planet or a binary star system)
⟶ Disk interaction
⟶ Combination of any of the above

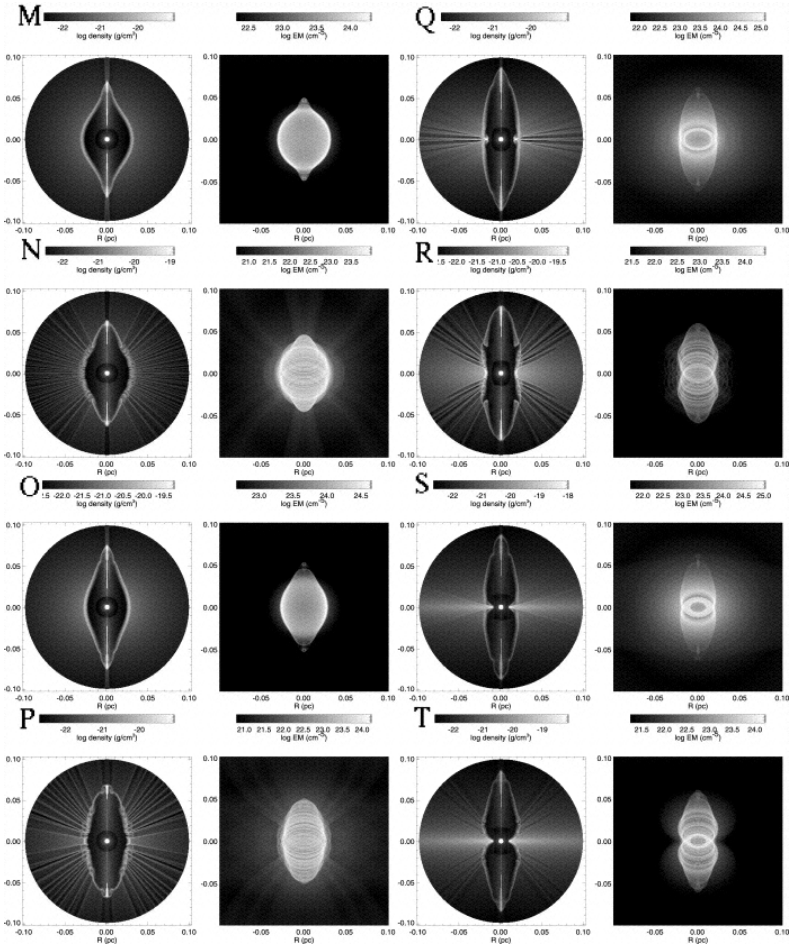

(Credit: Garcia-Segura et al. 1999)

Observations

. Five evolved stars:
OH231.8 (pPN),
IK Tau, IRC60370, AP Lyn (Miras),
RT Vir (semi-regular variable)

. VLBA, in Feb/Mar 2009

. H_2O masers at 22.235 GHz:
Rotational transition $6_{1,6} - 5_{2,3}$

. Low resolution: 128 channels of
0.104 km/s width, full polarization mode

. High resolution: 512 channels of
0.026 km/s width, dual polarization mode

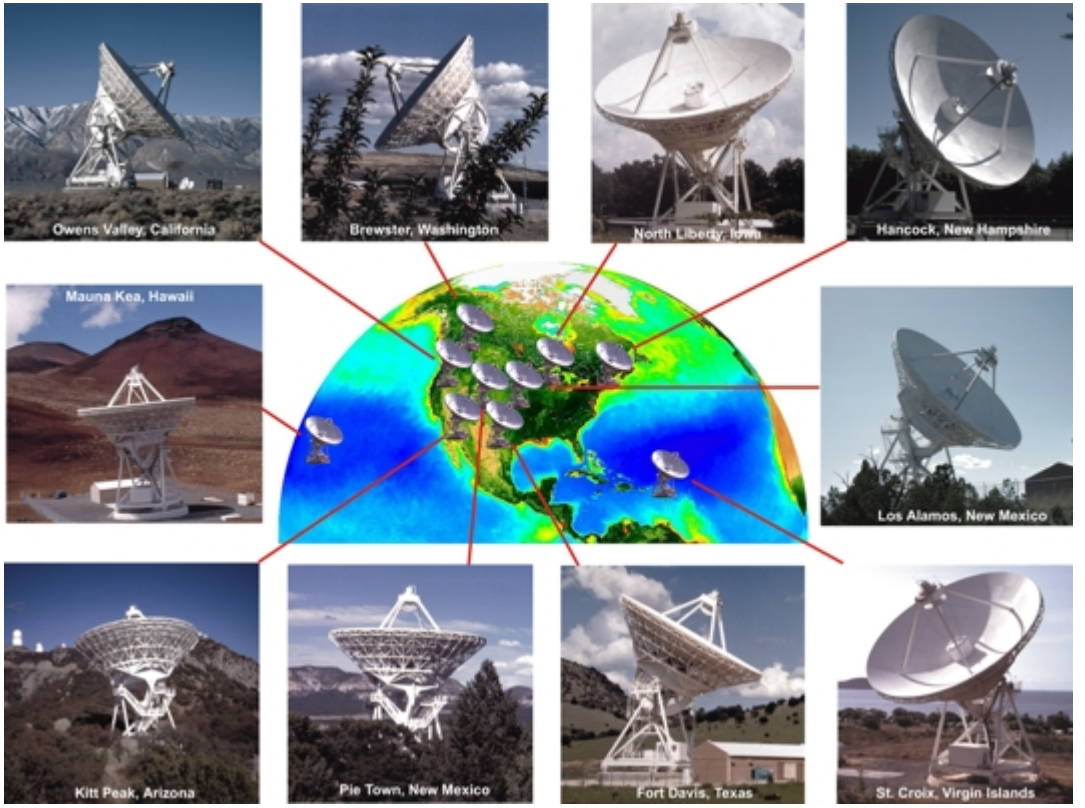

(Credit: NRAO/AUI/NSF)

Observations: Masers around Evolved Stars

. SiO masers:
⟶ At the extended atmosphere of the star; between the photosphere and the region where the dust is created.
⟶ Between ~2-3 AU (if R_{star} = 1 AU)

. OH masers:
⟶ At hundreds of AU from the star

. H_2O masers:
⟶ In between these 2 regions

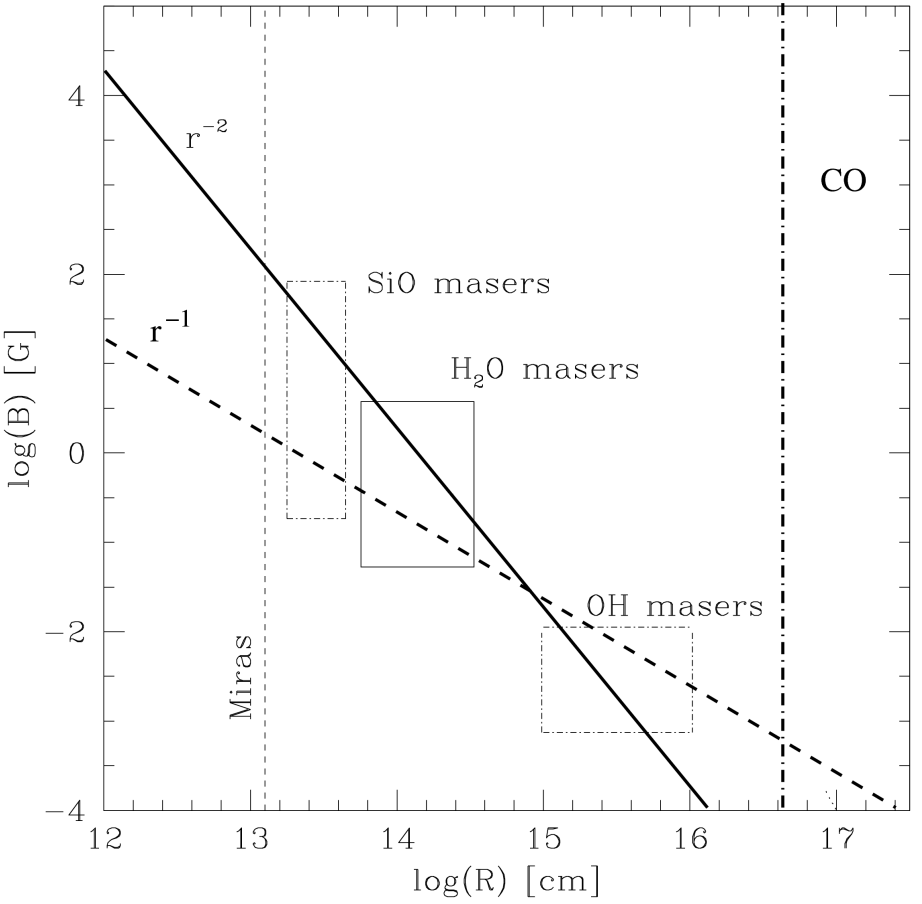

(Credit: Vlemmings; private communication)

Rotten Egg Nebula: Results

. Detection of 30 maser features*, composed by 252 maser spots
(*maser feature: when a maser spot survives the σ cut in at least 3 consecutive channels):

⟶ 20 features in the North Region
⟶ 10 features in the South Region

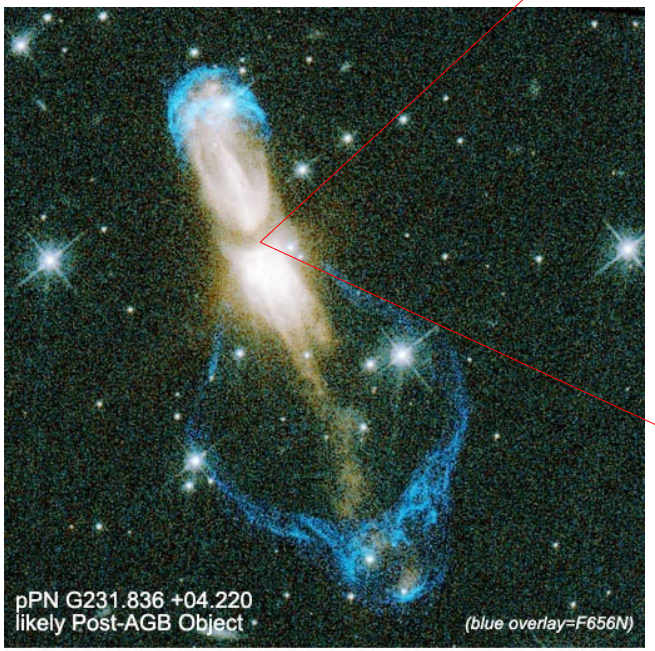

IRAS 07399-1435 [OH231.8+04.2, Rotten Egg, GLMP191] (4/2008)
07 42 16.83 -14 42 52.1 (2000), FOV=64.0", R:G:B = F814W:comb:F555W
WFPC2/WF3, credit PI:BUJARRABAL GO8326 NASA/ESA/STScI, Hubble Archives

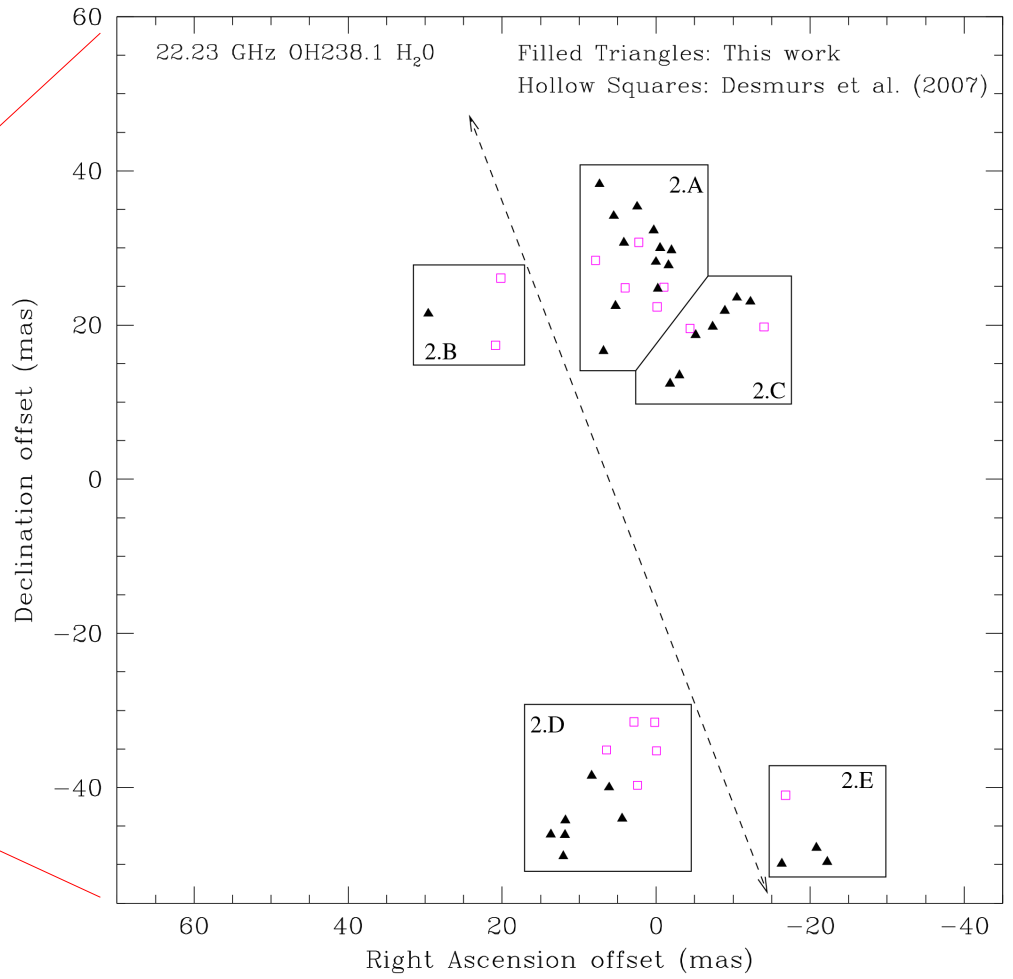

(Leal-Ferreira et al. 2012)

Rotten Egg Nebula: Results

. Detection of 30 maser features*, composed by 252 maser spots
(*maser feature: when a maser spot survive the σ cut in at least 3 consecutive channels):
⟶ 20 features in the North Region
⟶ 10 features in the South Region

. Comparing the positions of our detections and the observations of Desmurs et al. (2007), of regions 2.A and 2.D:
⟶ Adopting:
⟶ d = 1.54 kpc (Choi et al. 2011, updated from private communication)
⟶ i = 36° (Kastner et al. 1992, Shure et al. 1995)

V = 21 ± 11 km/s

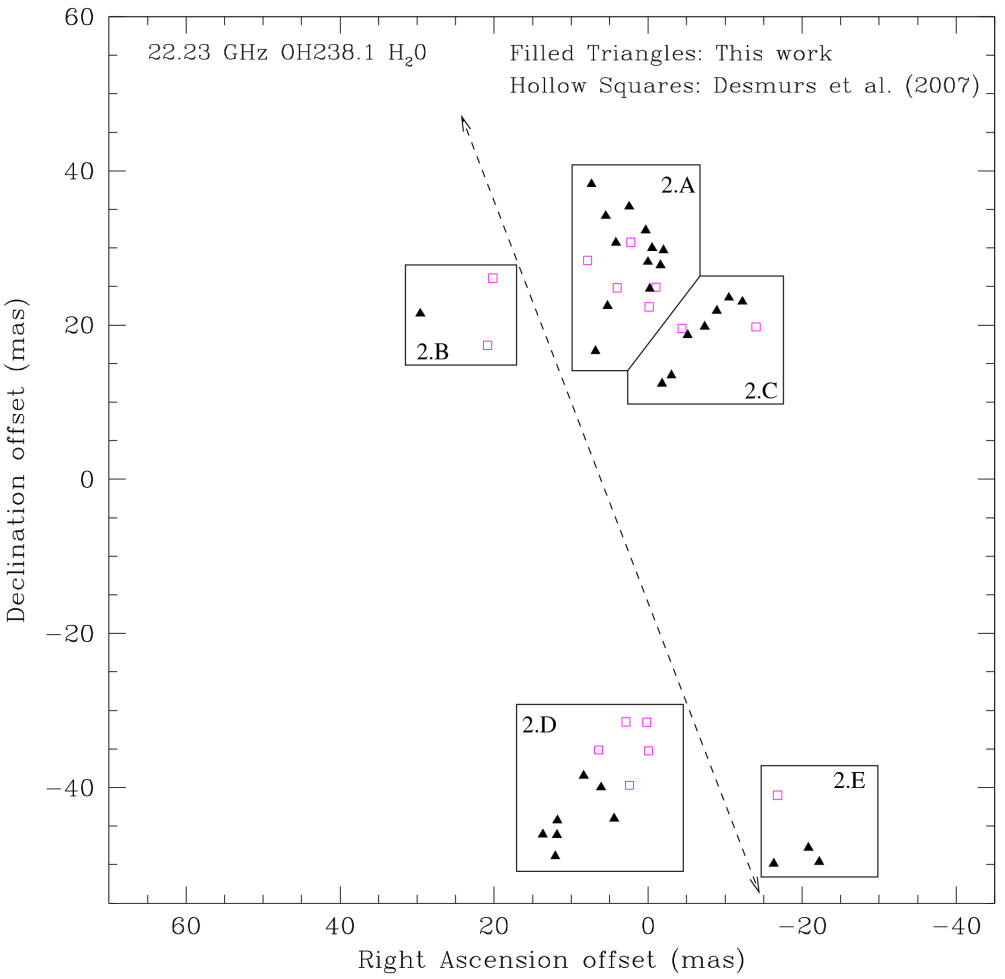

(Leal-Ferreira et al. 2012)

Rotten Egg Nebula: Results

. Detection of linear polarization in 3 features, all of them in the South Region

. EVPA scattering:

⟶ (i) Turbulence
⟶ (ii) Tangent points of a toroidal magnetic field
⟶ (iii) Internal Faraday Rotation (less likely)

Reg	Label	I (Jy/beam)	$\int$ I (Jy)	V_{lsr} (km/s)	POLI (%)	POLA (°)
SReg	S.05*	2.5472(+0)	3.5906(+0)	42.5	0.634 ± 0.003	-65.48 ± 5.73
SReg	S.06	1.3503(+0)	1.4570(+0)	41.9	1.148 ± 0.003	+58.00 ± 5.88
SReg	S.07	5.5267(+0)	6.7698(+0)	41.6	0.281 ± 0.002	-31.61 ± 3.72

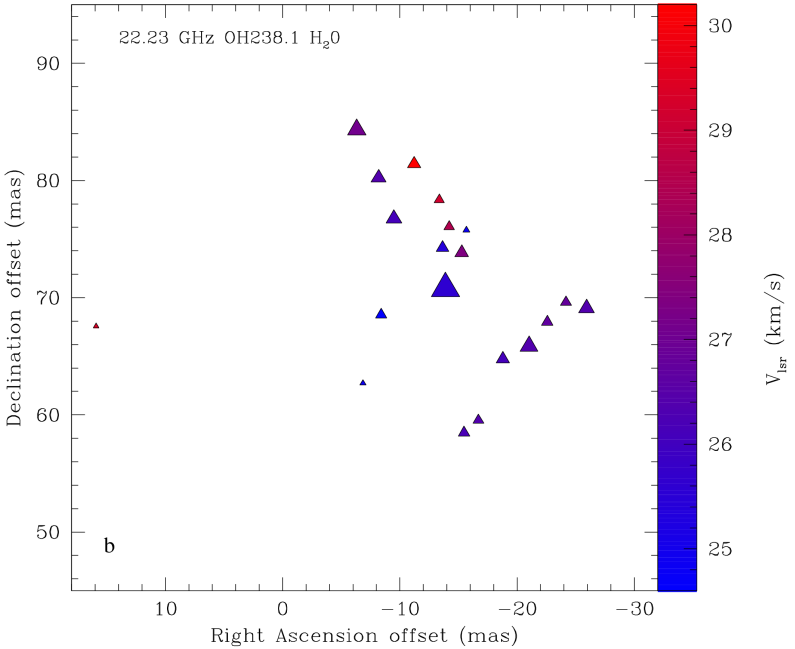

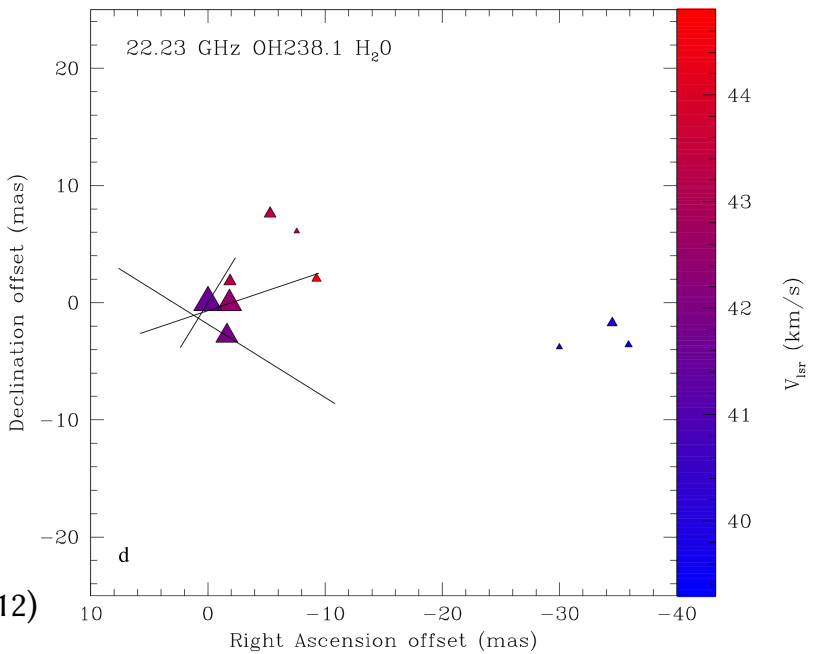

(Leal-Ferreira et al. 2012)

Rotten Egg Nebula: Results

. When circular polarization is present, the Stokes V spectrum should have a S-Shape

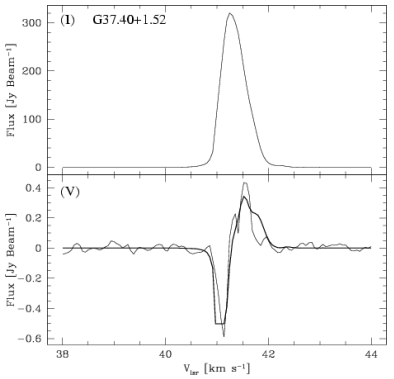

(Figure from Vlemmings et al. 2008)

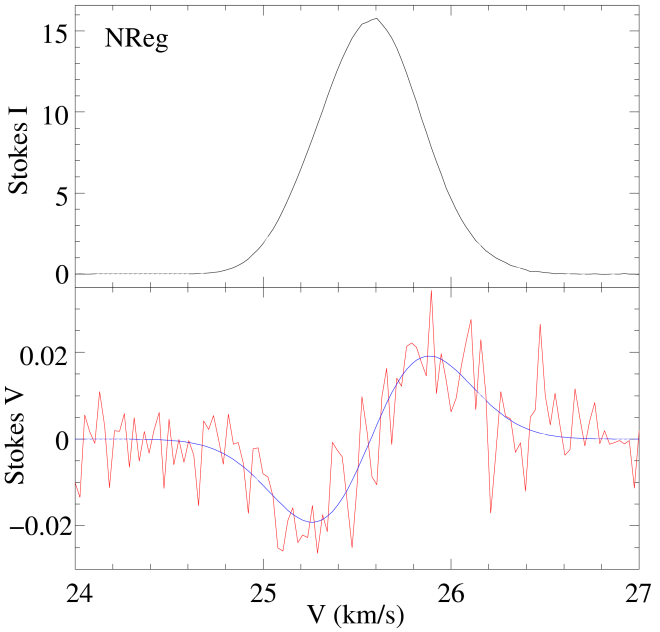

. Detection of circular polarization in 2 features, one in the South Region, one in the North Region

→ $B_{||}$ (North Region): 73 ± 11 mG

→ $B_{||}$ (South Region): -47 ± 34 mG

. Adopting $B \propto r^{-1}$: B_{star} = ~2.5 G

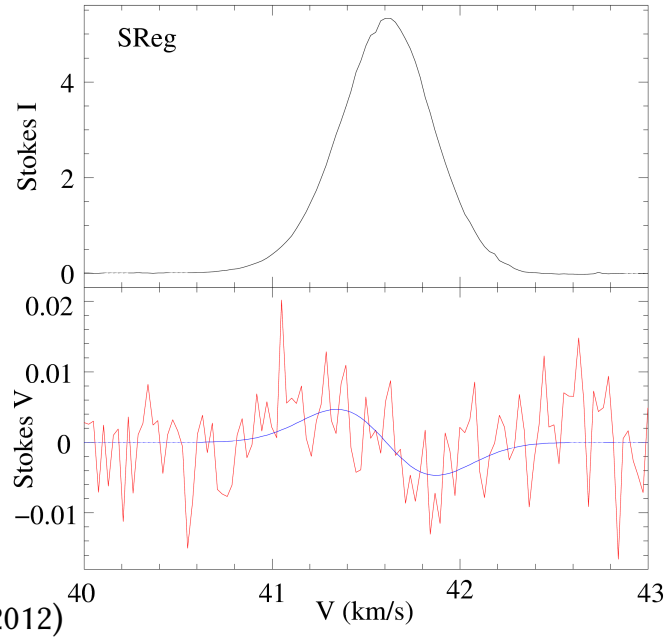

(Leal-Ferreira et al. 2012)

IK Tau: Results

. Detection of 85 maser features, composed by 525 maser spots

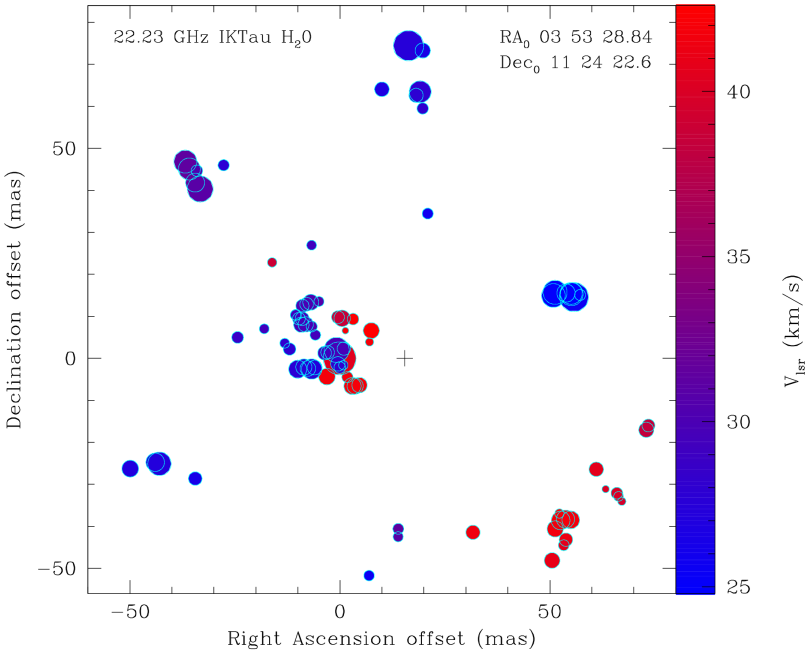

(Leal-Ferreira et al. 2012b, in prep.)

IK Tau: Results

. Detection of 85 maser features, composed by 525 maser spots

⟶ R_i = ~10 AU from the star

⟶ R_o = ~29 AU from the star

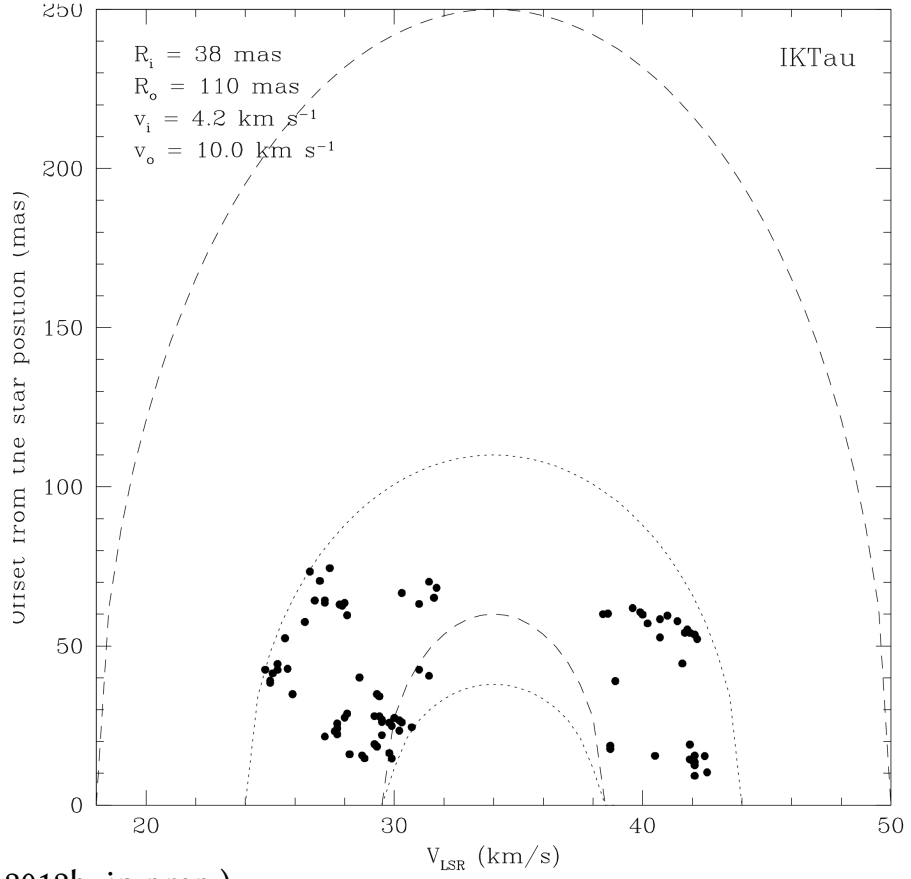

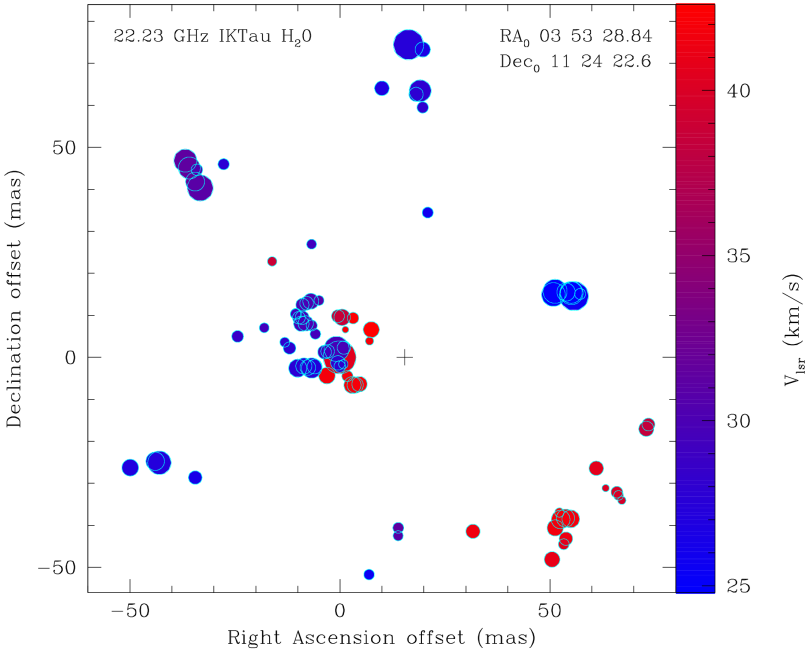

(Leal-Ferreira et al. 2012b, in prep.)

IK Tau: Results

. Detection of 85 maser features, composed by 525 maser spots

. Circular polarization on 3 features

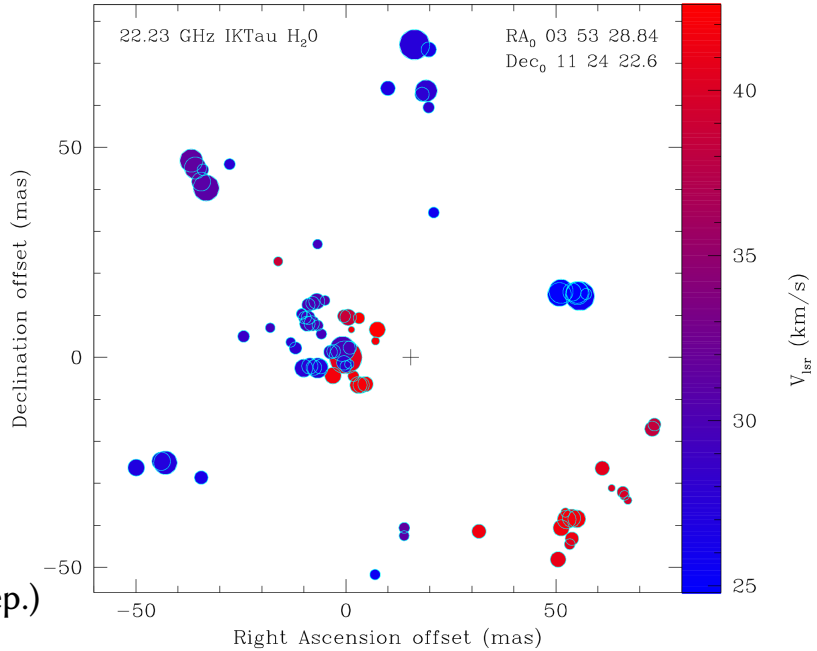

(Leal-Ferreira et al. 2012b, in prep.)

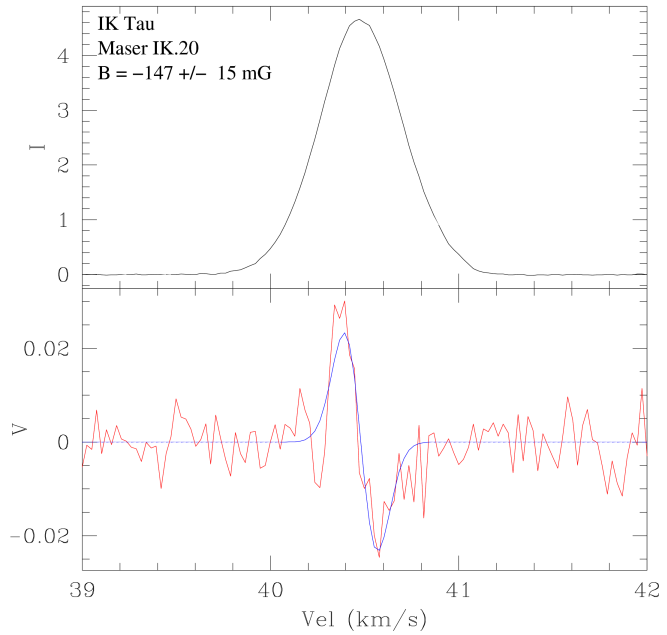

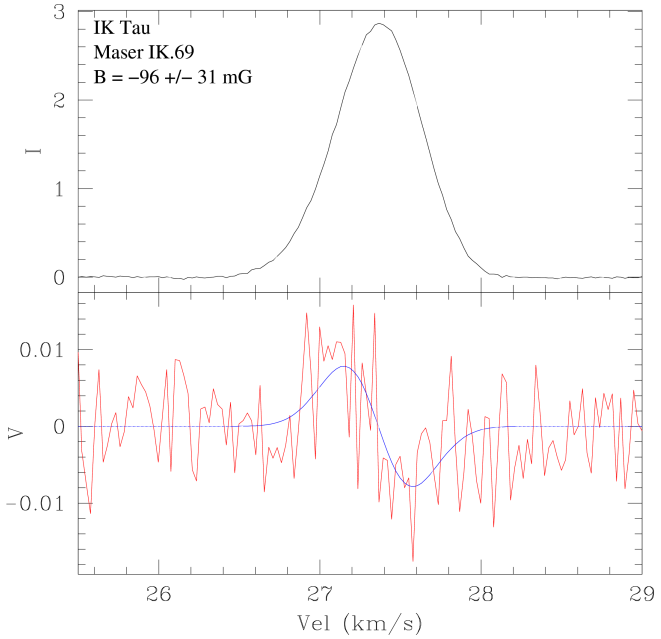

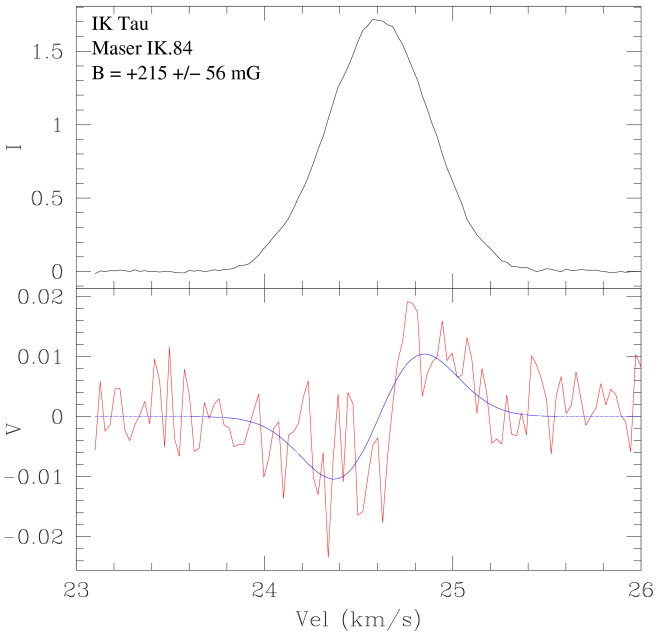

IK Tau: Results

. Detection of 85 maser features, composed by 525 maser spots

. Circular polarization on 3 features:

→ $B_{\parallel}$(IK.19) = -147 ± 15 mG

→ $B_{\parallel}$(IK.69) = -96 ± 31 mG

→ $B_{\parallel}$(IK.84) = 215 ± 56 mG

. If $B \propto r^{-1}$:

→ $0.65 < B_{star}[G] < 3.8$

. No linear polarization detection

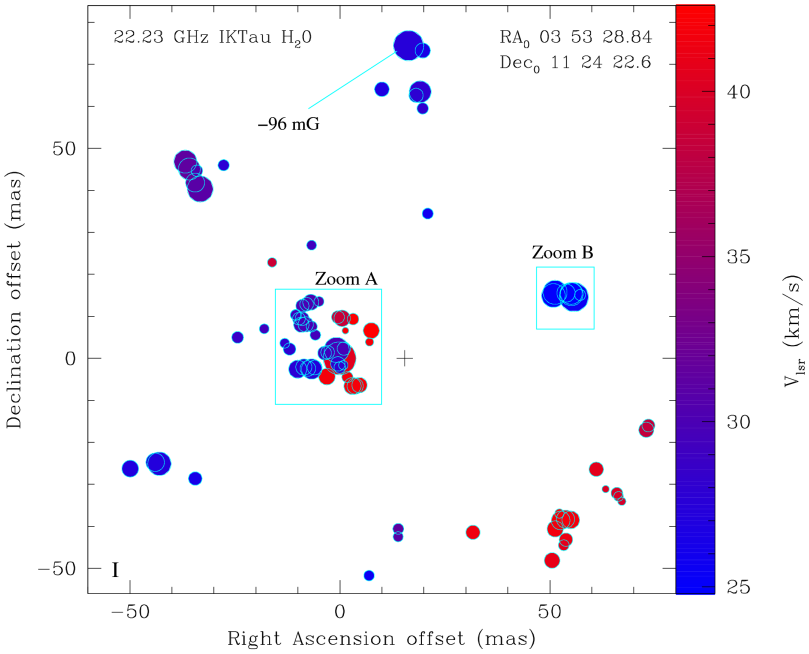

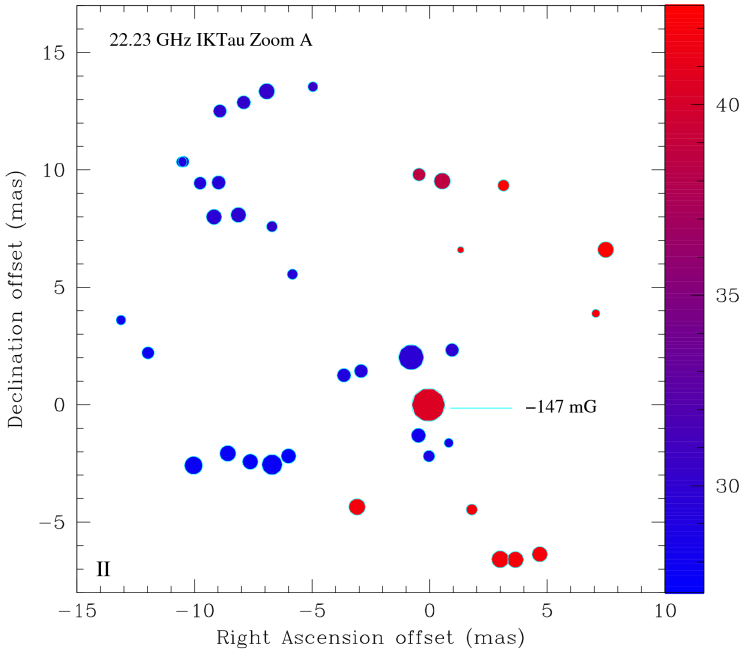

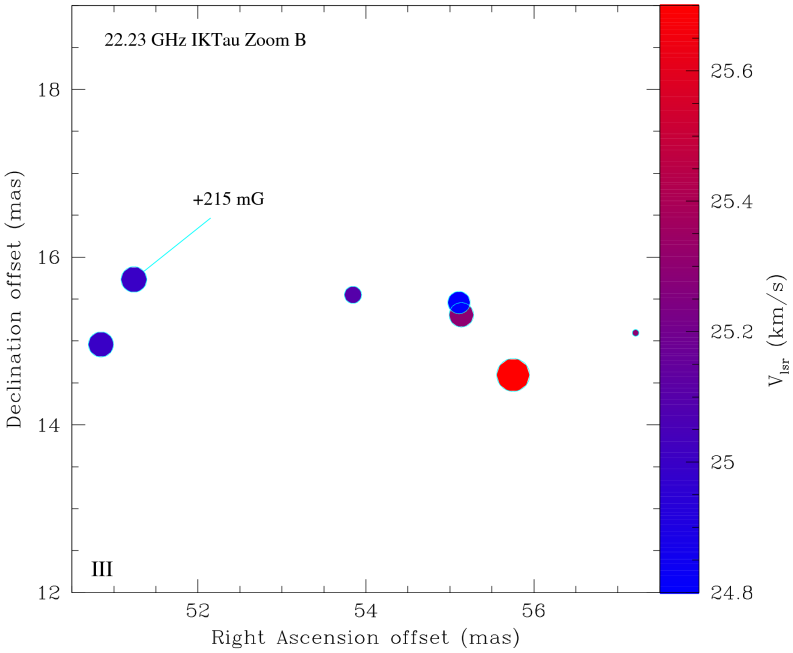

(Leal-Ferreira et al. 2012b, in prep.)

RT Vir, IRC 60370, AP Lyn: Summary

. RT Vir:

→ 91 maser features (from 671 maser spots)

→ Circular polarization on 2 (+1) features

→ $143 < |B_{\parallel}\ (\text{RT Vir})| \text{ [mG]} < 188$

→ If $B \propto r^{-1}$: $0.3 < B_{star}\ [\text{G}] < 2.9$

→ Linear polarization on 9 features

. IRC 60370

→ 62 maser features (from 634 maser spots)

→ Circular polarization on 5 features

→ $47 < |B_{\parallel}\ (\text{IRC 60370})| \text{ [mG]} < 331$

→ If $B \propto r^{-1}$: $0.25 < B_{star}\ [\text{G}] < 22$

→ Linear polarization on 9 features

. AP Lyn

→ No maser detection

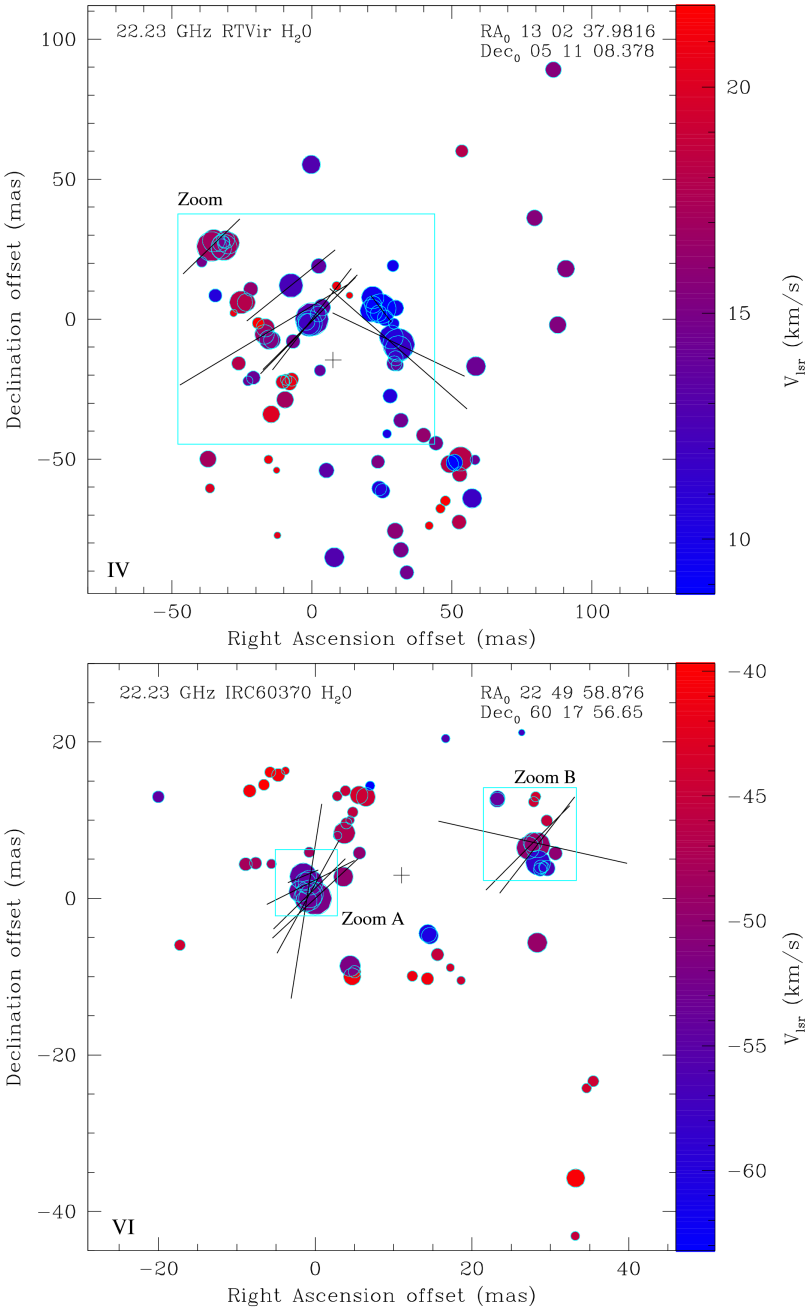

(Leal-Ferreira et al. 2012b, in prep.)

Discussion: Magnetic Field

. The magnetic field dependence is yet not well defined

⟶ But a $B \propto r^{-2}$ behavior looks more likely for IKTau.

⟶ With $B \propto r^{-2}$:

$6.6 < B_{iktau}[G] < 54.5$

. The observed magnetic field energy is similar or dominates the kinematic energy

⟶ $nKT\ (H_2O)\ [dyne/cm^2] \sim 10^{-5.2}$

⟶ $\rho\ V^2_{exp}\ (H_2O)\ [dyne/cm^2] \sim 10^{-4.1}$

⟶ $10^{-4.1} < B^2/8\pi\ (H_2O)\ [dyne/cm^2] < 10^{-2.4}$

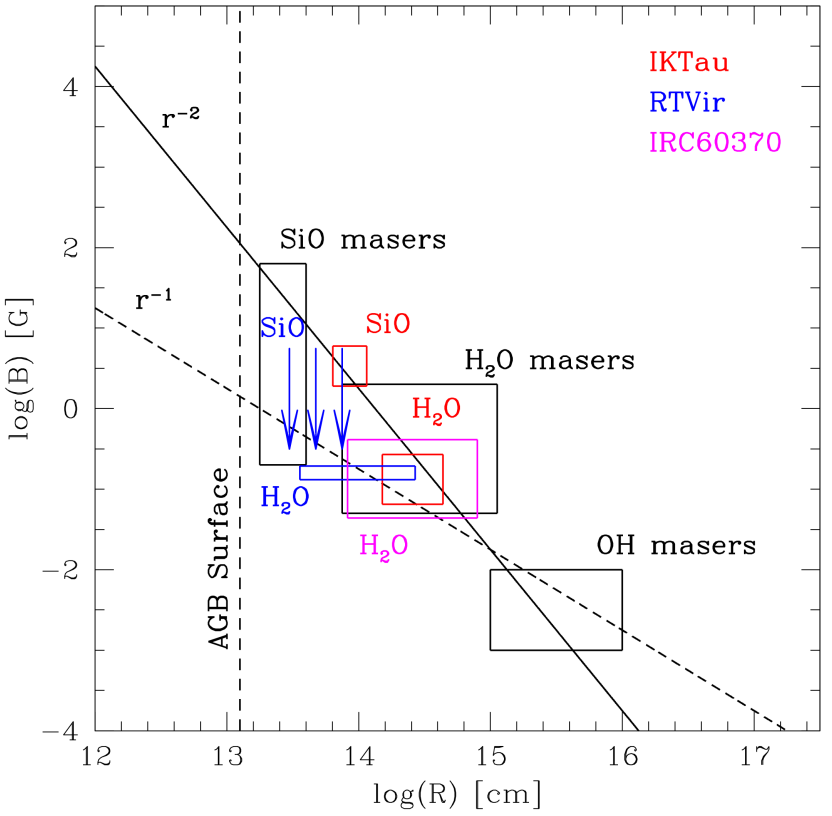

(Leal-Ferreira et al. 2012b, in prep.)

Conclusions

. We detected water masers in 4 of 5 sources

. A kinematic analysis in Rotten Egg Nebula shown that the masers are moving away with
⟶ v = 21 km/s

. Linear polarization was found in 3 of these 4 sources

. Circular polarization was found in all 4 sources

. We retrieved the magnetic field strength to be
⟶ 47 < B [mG] < 331 (± uncertainties) in the H_2O maser region

. We extrapolated the magnetic field strength to the surface of the stars, assuming $B \propto r^{-1}$:
⟶ 0.25 < B [G] < 22

. The dependence of B is not yet determined (IK Tau: $B \propto r^{-2}$ seems more likely). If that is so:
⟶ $6.6 < B_{iktau}[G] < 54.5$

. The observed magnetic energy can dominates the thermal/kinematic energy

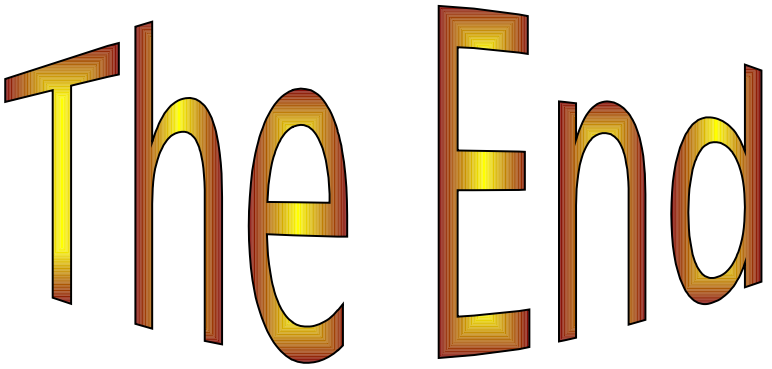
The End

Shaping Planetary Nebulae: Evidence of Magnetic Fields Around Evolved Stars

Marcelo L. Leal-Ferreira
(Argelander Institut für Astronomie, Germany)
Dr. Wouter H. T. Vlemmings
(Onsala Space Observatory, Sweden)

Argelander-Institut für Astronomie

DAAD

universitätbonn

Background: Artistic impression on W43A
Credit: NRAO/AUI/NSF

RT Vir: Results

. Detection of 91 maser features, composed by 671 maser spots

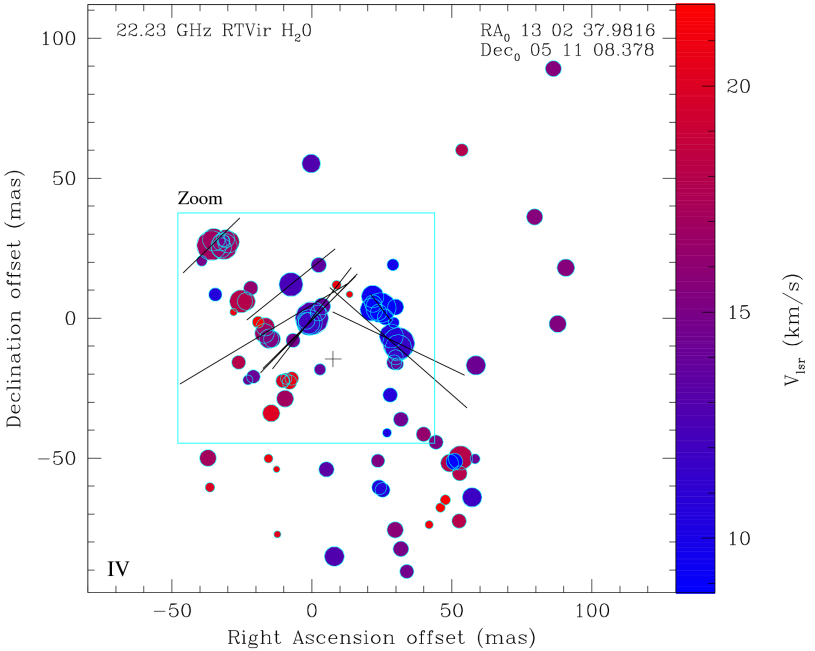

(Leal-Ferreira et al. 2012b, in prep.)

RT Vir: Results

. Detection of 91 maser features, composed by 671 maser spots

⟶ R_i = ~2.4 AU from the star

⟶ R_o = ~18 AU from the star

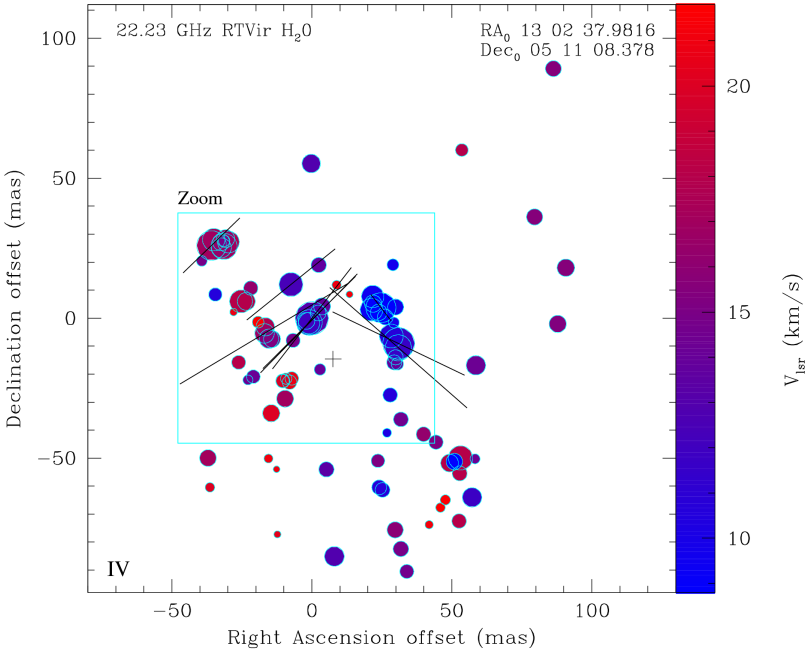

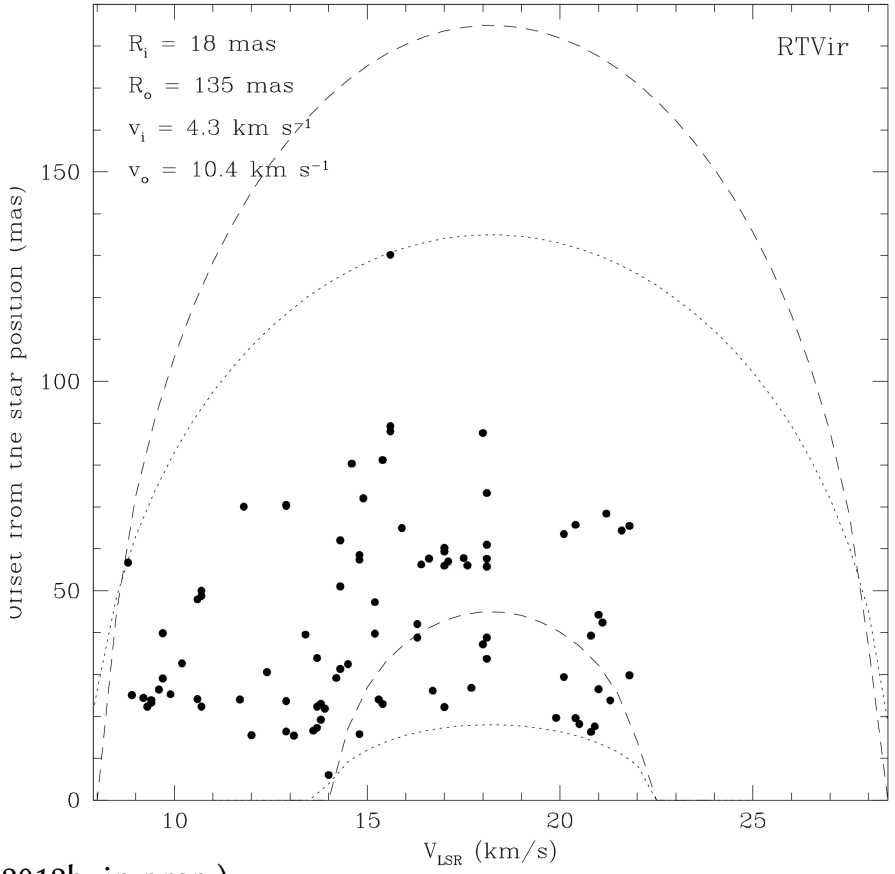

(Leal-Ferreira et al. 2012b, in prep.)

RT Vir: Results

. Detection of 91 maser features, composed by 671 maser spots

. Circular polarization on 3 features

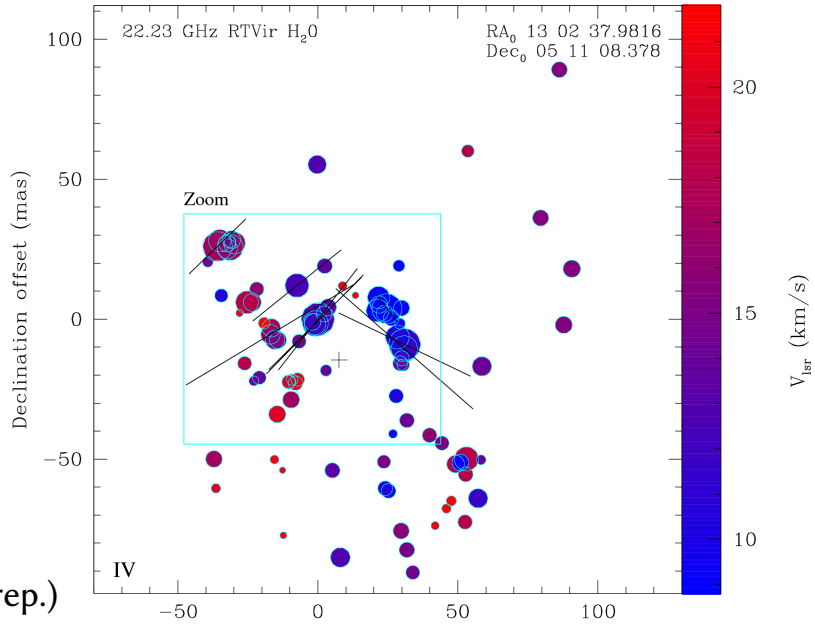

(Leal-Ferreira et al. 2012b, in prep.)

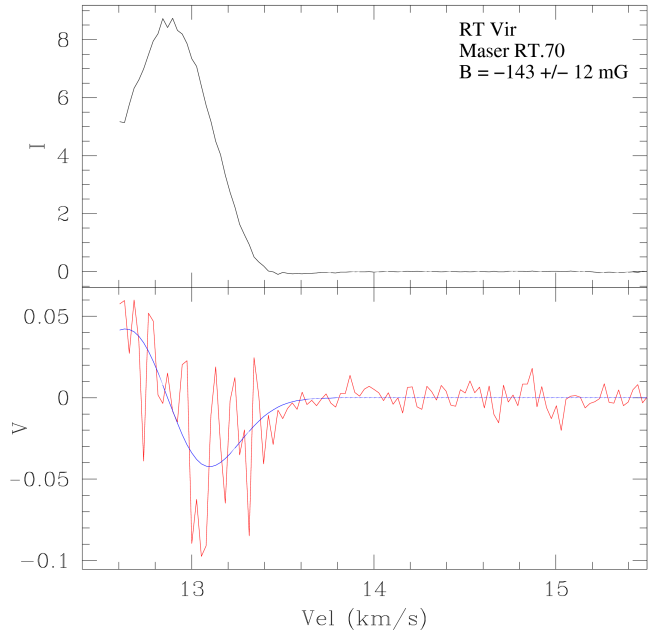

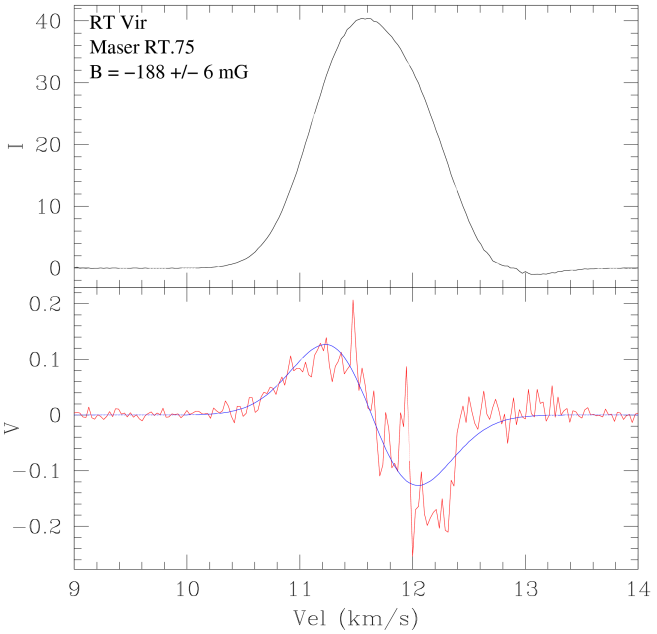

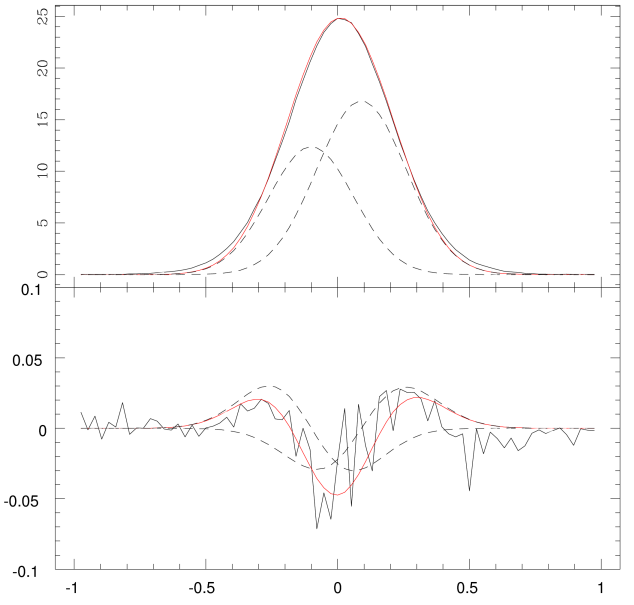

RT Vir: Results

. Detection of 91 maser features, composed by 671 maser spots

. Circular polarization on 3 features

$\longrightarrow B_{\parallel}$ (RT.70) = -143 ± 12 mG

$\longrightarrow B_{\parallel}$ (RT.75) = -188 ± 6 mG

$\longrightarrow B_{\parallel}$ (RT.90)* = -84 mG & +63 mG

*Not unique solution

. If $B \propto r^{-1}$:

$\longrightarrow 0.3 < B_{star}$ [G] < 2.9

. Linear polarization on 9 features

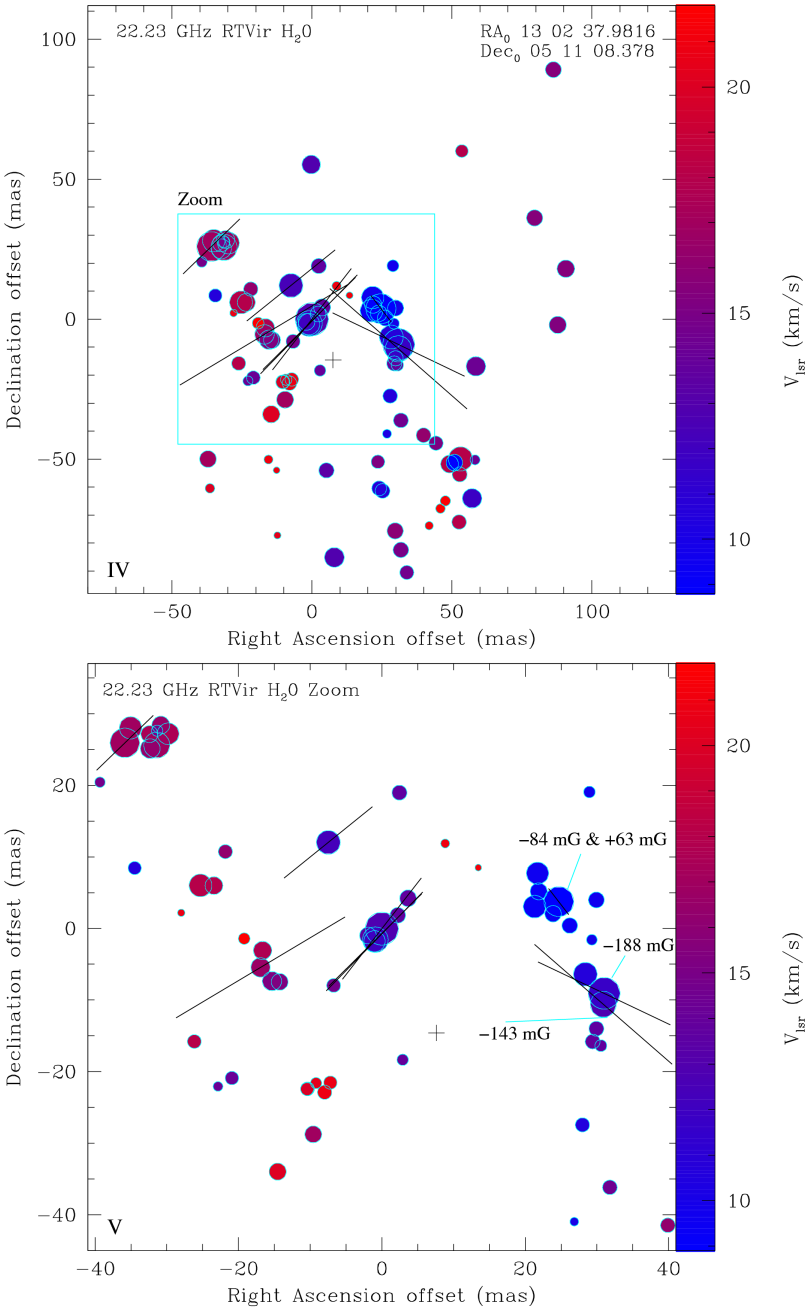

(Leal-Ferreira et al. 2012b, in prep.)

IRC 60370: Results

. Detection of 62 maser features, composed by 634 maser spots

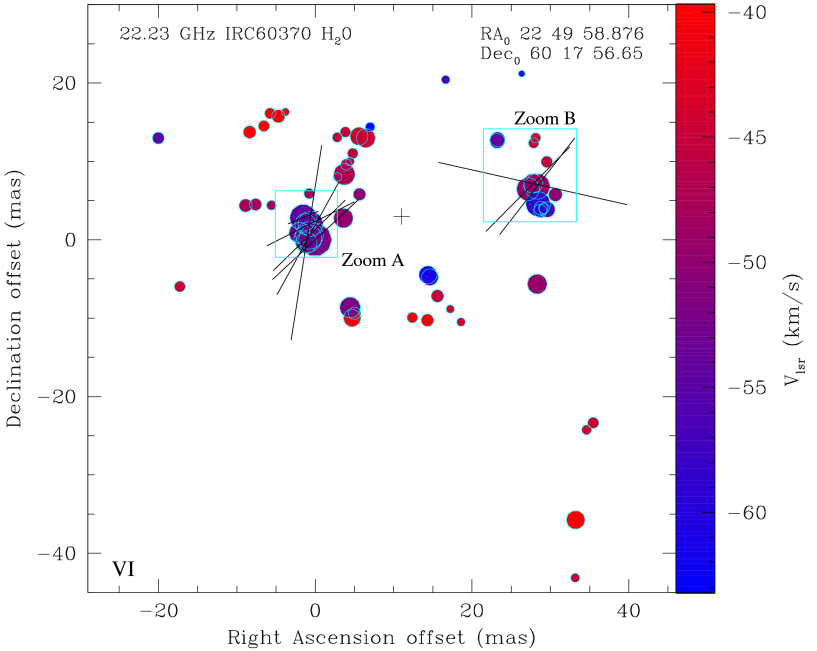

(Leal-Ferreira et al. 2012b, in prep.)

IRC 60370: Results

. Detection of 62 maser features, composed by 634 maser spots

⟶ R_i = ~5.5 AU from the star

⟶ R_o = ~53 AU from the star

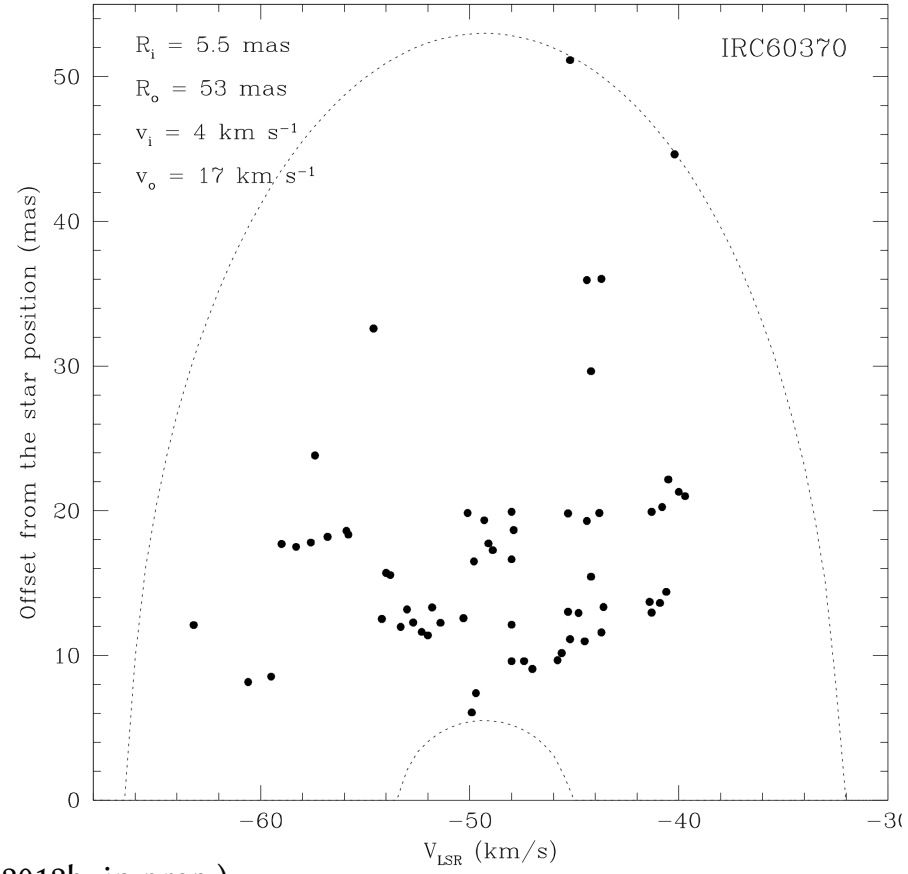

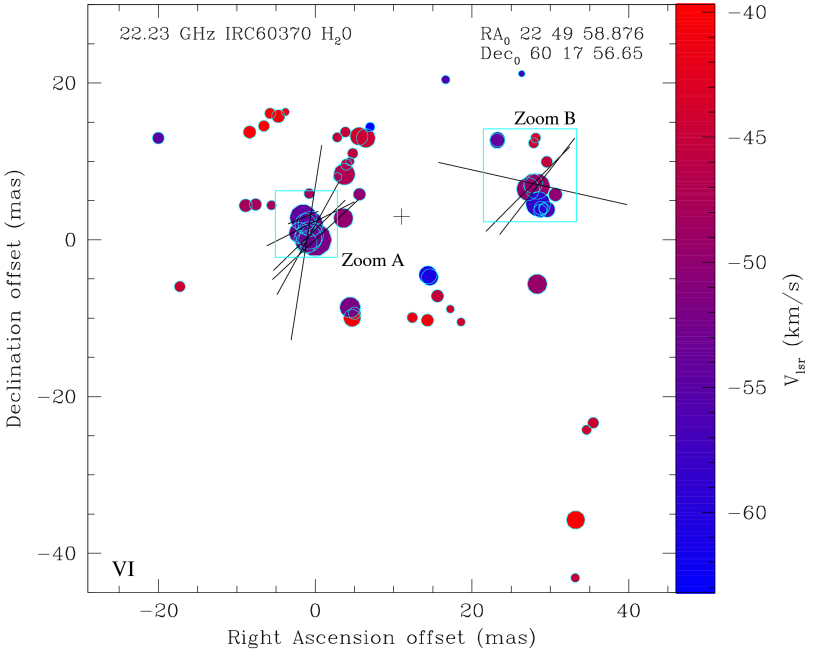

(Leal-Ferreira et al. 2012b, in prep.)

IRC 60370: Results

. Detection of 62 maser features, composed by 634 maser spots

. Circular polarization on 5 features

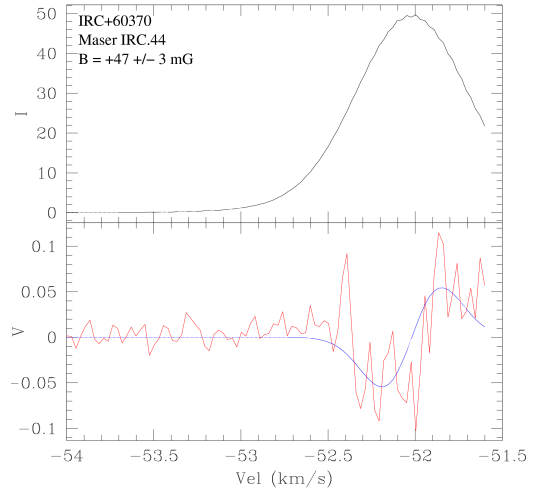

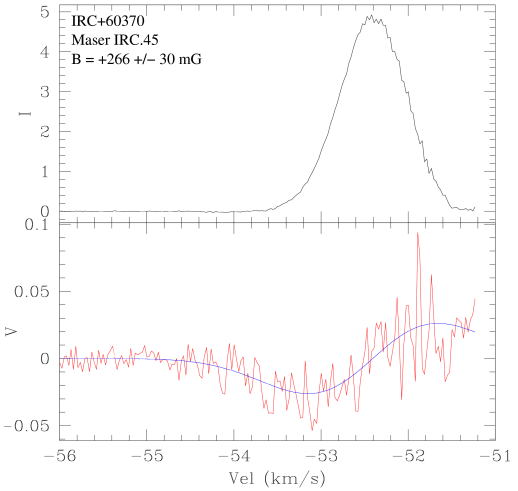

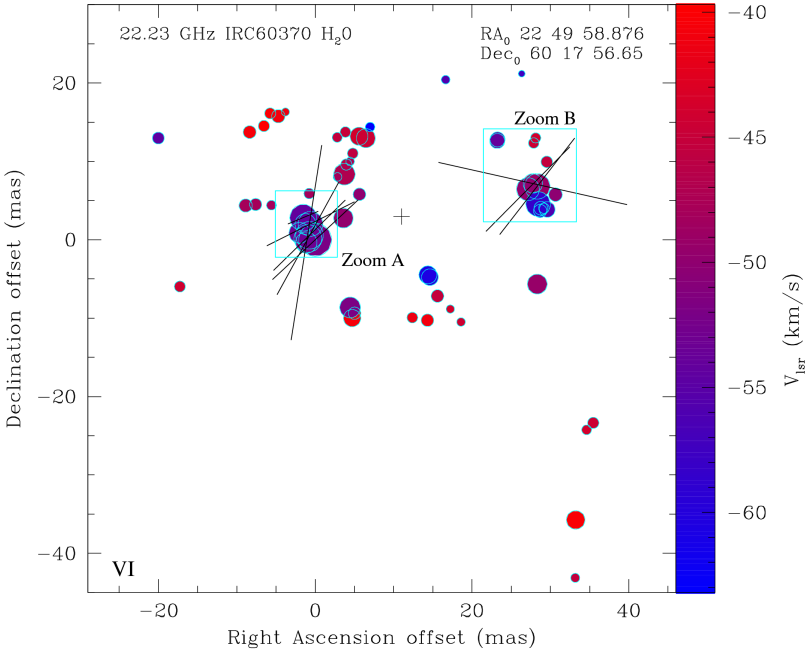

(Leal-Ferreira et al. 2012b, in prep.)

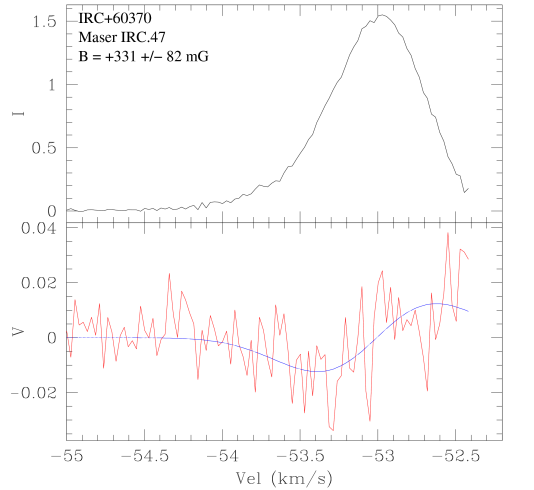

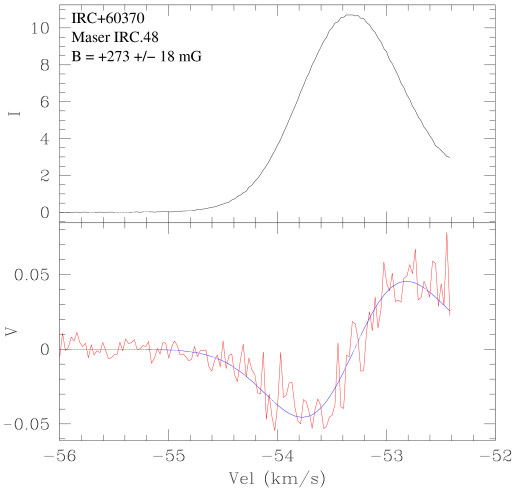

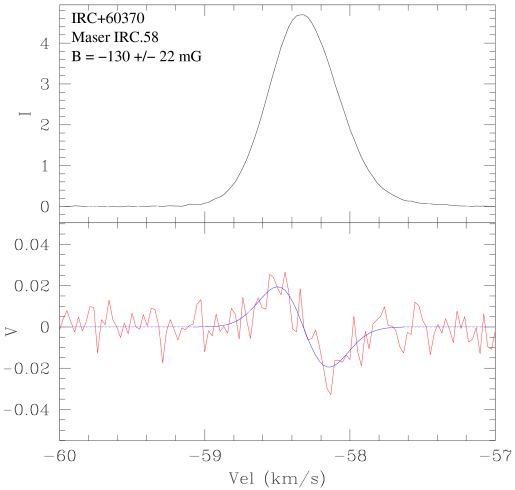

IRC 60370: Results

. Detection of 62 maser features, composed by 634 maser spots

. Circular polarization on 5 features

$\longrightarrow B_{\parallel}$ (IRC.44) = 47 ± 3 mG

$\longrightarrow B_{\parallel}$ (IRC.45) = 266 ± 30 mG

$\longrightarrow B_{\parallel}$ (IRC.47) = 331 ± 82 mG

$\longrightarrow B_{\parallel}$ (IRC.48) = 273 ± 18 mG

$\longrightarrow B_{\parallel}$ (IRC.58) = -130 ± 22 mG

.If $B \propto r^{-1}$:

$\longrightarrow 0.25 < B_{star}$ [G] < 22

. Linear polarization on 9 features

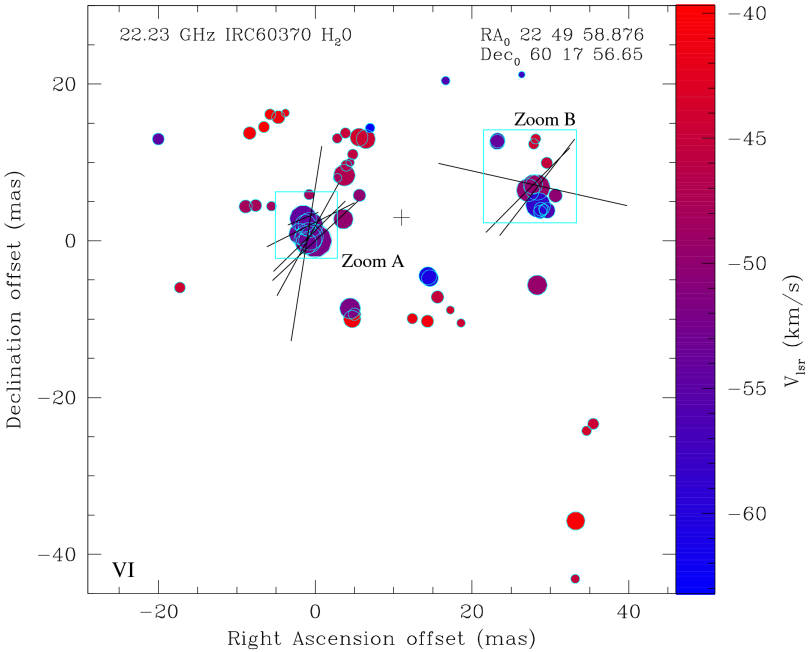

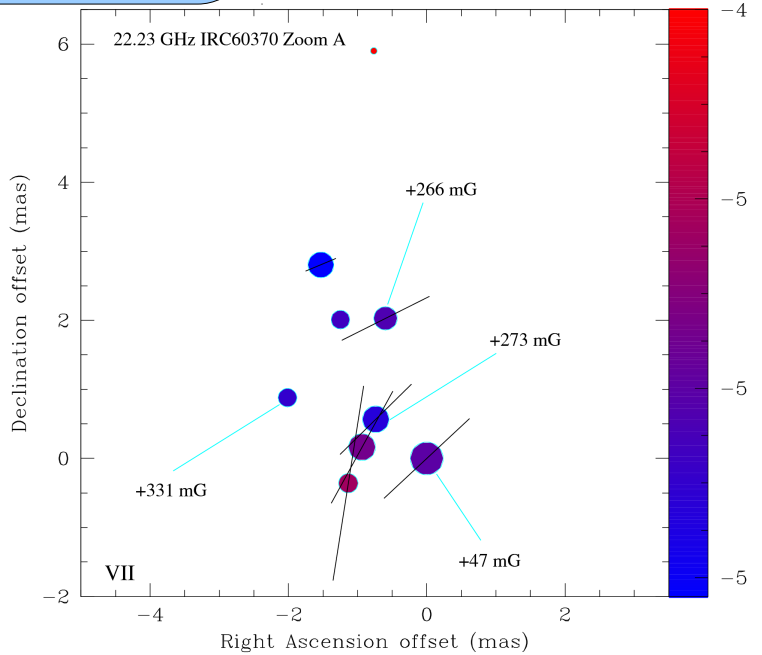

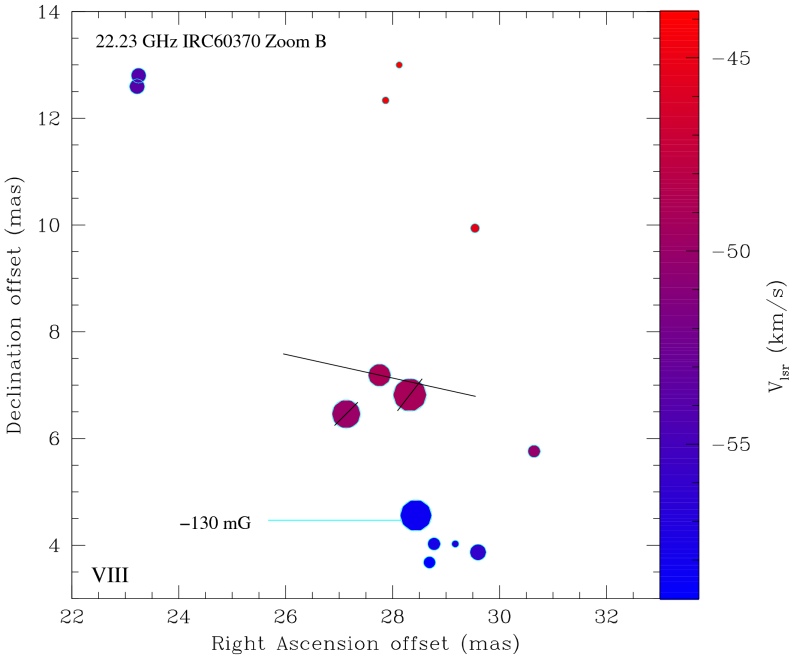

(Leal-Ferreira et al. 2012b, in prep.)